Mathematical Modeling of the Argon-Oxygen Decarburization Refining Process of Stainless Steel: Part II. Application of the Model to Industrial Practice

JI-HE WEI and DE-PING ZHU

The mathematical model proposed and presented in Part I of the present work has been used to deal with and analyze the austenitic stainless steel making (including ultralow-carbon steel) and has been tested on data of 32 heats obtained in producing 18Cr9Ni-grade steel in an 18-t argon-oxygen decarburization (AOD) vessel. The results indicated that the carbon concentrations and bath temperatures at the endpoints of blowing periods, calculated by the model, are in excellent agreement with the determined data, and the Cr content after the predeoxidization, obtained from the model predictions, also agrees very well with the observed value. The Gibbs free energies of the oxidation reactions of elements can be used to characterize fully the competitive oxidation among the elements during the refining process and to determine reasonably the corresponding distribution ratios of oxygen. The critical carbon concentration of decarburization (after which the decarburization changes to become controlled by the mass transfer of carbon in molten steel) for the AOD refining process of austenitic stainless steel in an 18-t AOD vessel is in the range of 0.25 to 0.40 mass pct. The model can provide some very useful information and a reliable basis for optimization of the technology of the AOD refining process of stainless steel and control of the process in real time and online.

A new mathematical model for the argon-oxygen decarburization (AOD) refining process of stainless steel was proposed and presented in Part I of the present work.[1] This model has been applied to the industrial practice of the austenitic stainless steel making (including ultralow-carbon steel) and tested on data of 32 heats obtained in producing 18Cr9Ni-grade steel in an 18-t AOD vessel, to examine its reasonability and reliability. The results are reported in this article.

I. APPLICATION OF THE MODEL TO INDUSTRIAL PRACTICE AND RESULTS

SOME of the related data of 32 heats obtained in producing 18Cr9Ni-grade austenitic stainless steel (including one heat of the ultralow-carbon steel) in an 18-t AOD vessel and the corresponding operations are given in Table I. The relevant total average absolute pressure in the bath for an 18-t AOD vessel (p_t) was 1.32 atm.

When the model is applied to a practical refining process, the remaining two parameters will be concerned. One is the utilization ratio of oxygen in the blowing process. It is fairly difficult to determine this parameter. This problem has been investigated by Gorges *et al.*[2] Referring to their results, the oxygen utilization ratios in the first, second, and third blowing periods for the refining process of austenitic stainless steel were, respectively, taken to be 0.90 to 0.95, 0.75 to 0.85, and 0.30 to 0.40 in the present work. Another parameter is the melting time of the added crop ends and scrap or alloy agents, *i.e.*, the time lapse of their cooling effect. It is just a research subject and has been reviewed by Oeters.[3] For simplicity, in the present work, based on the available theoretical and experimental studies and considering the flow and mixing characteristics in the AOD bath,[4] the melting time was taken to be 300 to 1200 seconds, according to their added amounts and the bath temperature at the time of addition. The concentrations of carbon and chromium and the temperatures at the endpoints of blowing periods predicted by the model, with the relevantly observed values of carbon content and bath temperature, are shown in Table II.

II. ANALYSIS AND DISCUSSION OF RESULTS

A. *Deviations of Results Predicted by the Model from Determined Values*

It can be seen from the data given in Table II that, so far, as the carbon concentrations and bath temperatures at the ends of blowing periods are concerned, the predicted results are in excellent agreement with the determined values. For period I of blowing, the maximum absolute deviations are 0.0083 mass pct and 15.84 K, and the relative mean deviations are 1.81 and 0.42 pct, respectively; for periods II and III of blowing, the maximum absolute deviations are 0.0014 mass pct and 7.59 K, 0.000 mass pct and 0.71 K, and the relative mean deviations are 1.21 and 0.13 pct, 0.00 and 0.035 pct, respectively. This indicates that the model can accurately predict the carbon contents and bath temperatures at the ends of blowing periods for the AOD refining process of stainless steel, and the reasonability and reliability of the model are fully confirmed.

Since the concentrations of Cr, Si, and Mn at the ends of blowing periods were not determined in production, the evaluations for the deviations of their values predicted by the model cannot be directly given. However, they can be

JI-HE WEI, Professor, is with the Department of Metallic Materials, Shanghai University, Shanghai, 200072, People's Republic of China. DE-PING ZHU, formerly Graduate Student, Department of Metallic Materials, Shanghai University, is Engineer, Shanghai Wensi Sorftware Limited Company.

Manuscript submitted January 9, 2001.

Table I. Relevant Data and Operations for Refining Process of Austenitic Stainless Steel in an 18-t AOD Vessel*

Heat	Initial Mass of Steel, t	Initial Temperature, K	Initial Composition of Steel, Mass Pct				Cumulative Time, min	I Period of Blowing		Amount of addition agent, t	II Period of Blowing	
			C	Cr	Si	Mn		O_2 Flowrate, Nm^3/h	N_2 Flowrate, Nm^3/h**		O_2 Flowrate, Nm^3/h	Ar Flowrate, Nm^3/h**
266	19.4	1782	1.12	16.74	0.18	0.23	0 13 34 47.25	800	400	lime, 0.20 (1),0.70;(2),0.17	600	600
268	18.5	1791	1.12	18.25	0.19	0.24	0 16 26.5 35.85	800	400	lime, 0.20 (1),0.1;(2),0.06;(3)0.5	600	600
278	18.2	1815	1.12	17.75	0.24	0.27	0 13 27.5 28.5 38	800	400	lime, 0.20 (1),0.35;(2),0.08 (3),0.5	600	600
281	19.45	1806	1.23	17.60	0.23	0.28	0 9 26 36.75	800	400	lime, 0.20 (1),0.15;(2),0.08	600	600
283	19.65	1788	0.96	17.61	0.33	0.23	0 10 24.2 38	800	400	lime, 0.20 (1),0.6;(2),0.02	600	600
294	19.15	1793	1.78	16.74	0.22	0.25	0 7 34.75 46.7	800	400	lime, 0.20 (1),0.6;(2),0.02	600	600
297	19.5	1804	0.86	17.84	0.26	0.33	0 8 21 33.85	800	400	lime, 0.20 (1),0.15;(2),0.07	600	600
300	17.1	1795	0.96	16.97	0.21	0.25	0 14 22 33.85	800	400	lime, 0.20 (1),0.35;(2),0.04;(4),0.05	600	600
305	18.5	1820	0.72	17.80	0.26	0.32	0 7 23.5 24 33.75	800	400	lime, 0.20 (1),0.25 (3),0.30	600	600
307	18.8	1830	0.95	17.63 0.36 Mo	0.32	0.79	0 16 22 35.5 47	800	400	lime, 0.20 (2),0.07;(4),0.64	480	680
										III period of blowing →	(240)	(920)
343	18.1	1879	0.83	16.71	0.15	0.23	0 6 24.15 25 37.65	800	400	lime, 0.20 (1),0.7;(2),0.06	600	600
353	20.6	1797	1.40	16.85	0.20	0.40	0 11 36.4 50	800	400	lime,0.20 (1),0.4;(2),0.1	600	600
354	19.8	1815	1.21	17.44	0.24	0.33	0 16.5 29.3 39	800	400	lime,0.20 (1),0.4;(2),0.2	600	600
355	19.0	1830	1.11	17.63	0.21	0.33	0 8 23 37	800	400	lime,0.20 (1),0.2;(2),0.07	600	600

Table I. Continued. Relevant Data and Operations for Refining Process of Austenitic Stainless Steel in an 18-t AOD Vessel*

Heat	Initial Mass of Steel, t	Initial Temperature, K	Initial Composition of Steel, Mass Pct C	Cr	Si	Mn	Cumulative Time, min	I Period of Blowing O_2 Flowrate, Nm^3/h	N_2 Flowrate, Nm^3/h**	Amount of addition agent, t	II Period of Blowing O_2 Flowrate, Nm^3/h	Ar Flowrate, Nm^3/h**
356	19.6	1795	1.12	17.21	0.30	0.28	0 15 27 38.75	800	400	lime,0.20 (1),0.4;(2),0.08	600	600
357	19.4	1780	0.80	17.22	0.25	0.32	0 13 24 43.5	800	400	lime,0.20 (1),0.4;(2),0.1;(4),0.15	600	600
358	19.4	1792	1.13	17.69	0.22	0.30	0 12 25 38.7	800	400	lime,0.20 (1),0.15;(2),0.12	600	600
370	18.8	1820	1.31	18.26	0.36	0.26	0 30 31 38.15	800	400	lime,0.20 (3),0.4;(2),0.05	600	600
371	18.4	1821	1.06	18.30	0.29	0.31	0 20.15 21 37.85	800	400	lime,0.20 (2),0.06;(3),0.7	600	600
379	18.4	1813	1.03	18.17	0.16	0.29	0 22 23 36	800	400	lime,0.20 (2),0.06;(3),0.8	600	600
381	18.2	1824	1.25	18.05	0.28	0.32	0 12 30 40.5	800	400	lime,0.20 (1),0.1;(2),0.06;(3),0.03	600	600
382	18.0	1808	1.00	17.56	0.21	0.31	0 14 25.5 40.5	800	400	lime,0.20 (1),0.3;(2),0.05;(3),1.0	600	600
393	19.3	1804	1.41	17.18	0.15	0.20	0 13.5 31 43.5	800	400	lime,0.20 (1),0.55;(2),0.15	600	600
394	18.9	1787	1.56	17.23	0.22	0.22	0 13 35 45.5	800	400	lime,0.20 (1),0.4;(3),0.3	600	600
395	18.8	1793	1.40	17.29	0.29	0.23	0 17 37 46.5	800	400	lime,0.20 (1),0.35;(2),0.15	600	600

*The data and operations of only 25 heats are included here for saving space.
**The total gas flow rate of two subtuyeres was 200 Nm^3/h.
†(1) High-carbon Fe-Cr, (2) Ni plate, (3) Crop ends or scrap, and (4) High-carbon Fe-Mn.

indirectly examined using the determined data regarding the composition of the molten steel and slag melt after the predeoxidization compared with the model predictions for the composition of the slag melt and the amounts of steel and slag at the end of blowing period II. Taking heat 354 as a example, as a result of the predeoxidization treatment just after the end of blowing period II, the observed Cr concentration of the liquid steel was 17.74 mass pct and the Cr_2O_3 content in the slag was 16.53 mass pct. The concentrations of Cr and Cr_2O_3 at the end of blowing period II, given by the model, were 16.64 and 35.80 mass pct, and the relevant amounts of the steel and slag were 19,593 and 1824 kg, respectively. According to these and by mass balance, it can be obtained that the Cr content in the steel after the predeoxidization would be 17.87 mass pct, which agrees, again, excellently with the determined value. This verifies further the reasonability and reliability of the model.

B. *Competitive Oxidation of Elements and Distribution Ratios of Blown Oxygen among Elements*

As mentioned before, there must exist the competitive oxidation of various elements in the AOD refining process

Table II. Some Results Predicted by the Model and Plant Data

	End of I period					End of II Period				
	[C], Mass Pct		[Cr], Mass Pct	Bath Temperature, K		[C], Mass Pct		[Cr], Mass Pct	Bath temperature, K	
Heat	Predicted	Determined	Predicted	Predicted	Determined	Predicted	Determined	Predicted	Predicted	Determined
266	0.1914	0.19	16.5402	1975.42	1975	0.0304	0.03	15.7215	2054.55	2055
267	0.1714	0.17	17.5504	1996.18	1984	0.0414	0.04	17.0978	2043.05	2037
268	0.1806	0.18	16.8876	1968.29	1962	0.0504	0.05	16.4988	2014.95	2014
278	0.1737	0.17	17.2656	1993.19	1983	0.0606	0.06	17.1655	2022.70	2021
279	0.2370	0.23	17.1447	1961.04	1947	0.0409	0.04	16.2985	2056.13	2056
281	0.2030	0.20	16.8131	1992.92	1991	0.0405	0.04	16.2744	2058.48	2058
282	0.1930	0.19	16.9879	1989.12	1985	0.0608	0.06	16.6313	2038.85	2038
283	0.2059	0.20	16.8217	1971.14	1966	0.0603	0.06	16.1588	2048.33	2048
293	0.2230	0.22	17.2685	1966.05	1954	0.0509	0.05	16.7699	2027.97	2023
294	0.1954	0.19	16.6261	1972.66	1965	0.0503	0.05	15.7643	2067.78	2067
295	0.1952	0.19	16.8209	1959.28	1946	0.0606	0.06	15.9046	2056.16	2056
297	0.2130	0.21	17.1817	1980.47	1972	0.0404	0.04	16.4673	2061.07	2057
299	0.1617	0.16	16.6702	2001.81	1992	0.0512	0.05	16.1538	2059.52	2059
300	0.2270	0.22	16.5685	1966.34	1963	0.0502	0.05	15.7690	2060.52	2061
305	0.1545	0.15	17.0826	1994.44	1986	0.0504	0.05	16.5093	2040.47	2039
306	0.1702	0.17	17.7453	1989.30	1989	0.0603	0.06	17.2697	2026.06	2026
307*	0.1729	0.17	16.1699	1968.25	1965	0.0301	0.03	15.8966	2018.83	2018
343	0.1817	0.18	17.2903	1957.28	1949	0.0404	0.04	16.7015	2022.90	2019
353	0.2046	0.20	16.9699	1956.33	1946	0.0405	0.04	16.3041	2033.67	2028
354	0.1806	0.18	17.0972	1985.25	1984	0.0506	0.05	16.6369	2044.31	2044
355	0.1841	0.18	17.0828	1979.50	1971	0.0601	0.06	16.5633	2046.39	2043
356	0.2209	0.22	17.1454	1960.74	1960	0.0603	0.06	16.6965	2016.54	2016
357	0.2212	0.22	16.5266	1954.57	1950	0.0405	0.04	15.8086	2057.89	2056
358	0.2239	0.23	16.8101	1967.76	1967	0.0509	0.05	16.0966	2052.43	2048
370	0.1220	0.12	17.6135	2049.26	2046	0.0605	0.06	17.1419	2053.20	2048
371	0.2035	0.20	17.8770	1967.57	1960	0.0505	0.05	17.0333	2014.89	2013
379	0.1583	0.15	17.0306	1991.38	1979	0.0513	0.05	16.7107	2030.59	2023
381	0.1379	0.13	17.1643	1961.36	1954	0.0510	0.05	16.2768	2061.11	2051
382	0.2429	0.24	16.6511	1945.86	1945	0.0509	0.05	15.8977	2033.68	2033
393	0.1954	0.19	16.8539	1968.84	1953	0.0408	0.04	16.2836	2032.65	2025
394	0.1526	0.15	16.9838	1990.76	1989	0.0505	0.05	16.3941	2046.19	2046
395	0.1509	0.15	16.6921	1990.75	1977	0.0504	0.05	16.2962	2037.96	2032

*At the end of the III blowing period, the corresponding predicted results were 0.02 mass pct C, 15.7782 mass pct Cr, and 2009.71 K, and the determined values were 0.02 mass pct C and 2009 K, respectively.

of stainless steel, like that in any multicomponent reaction system. The blown oxygen has different distribution ratios among elements, and the ratios will dynamically change with the refining conditions, particularly the composition and temperature of the bath. In the present work, the Gibbs free energies of various oxidation reactions were first used to try to determine the values of this parameter for the elements. The distribution ratios of blown oxygen among C, Cr, Si, and Mn dissolved in the molten steel for three heats (No. 266, 281, and 354) are shown in Figure 1.

According to the results predicted by the model, it should be said that this way is entirely reasonable and feasible. At the initial stage of the refining, the bath temperature is lower, the blown oxygen is primarily consumed for the losses of Si, Cr, and Mn, and the ratio of oxygen consumed for decarburization is only approximately 20 to 30 pct (dependent on the initial temperature of the liquid steel). With the blowing process progressing, the bath temperature gradually heightens and the total ratio of oxygen occupied by Cr, Si, and Mn gradually decreases; however, x_{Si} still enlarges and x_C continuously increases. With the bath temperature rising and the concentrations of the elements reducing further, a dynamic equilibrium of (usually first) the Mn, then Si, oxidation reaction is attained; correspondingly, x_{Mn} and x_{Si} nonsynchronously approach zero. After this, the supplied oxygen mainly distributes between C and Cr. The maximum of x_C can approach 60 to 86 pct at the later stage of blowing period I, depending upon the bath conditions. After having reached the maximum point, with the blowing process continuously progressing, x_C uninterruptedly decreases and x_{Cr} constantly increases. At the end of blowing period II, x_C is about 10 to 15 pct. The bath temperature can strongly influence the distribution of oxygen. At the initial moment of the blowing, the value of x_C for heat 266 is markedly less than that for heat 354 and is also less than that for heat 281, the most important reason being the low initial temperature of its liquid steel, only 1782 K.

It is necessary to point out that after x_{Si} and x_{Ma} are equal to zero, manganese and silicon are still taking part in the oxidation-reduction reactions in the system and influence the distribution of oxygen between carbon and chromium, although they no longer consume oxygen. Under a certain condition, a small amount of MnO or SiO_2 may even be reduced, and appropriately, x_{Mn} or x_{Si} possesses a minus value (Figure 1).

It should also be emphasized that the values of x_i given in the present work are determined not only by the Gibbs free energies of oxidation reactions, but also by the effects

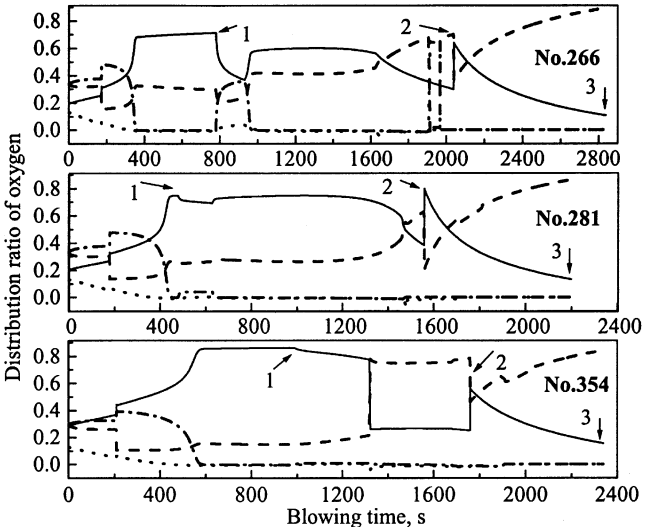

Fig. 1—Distribution ratios of blown oxygen among C, Cr, Si, and Mn during the refining process: C —— Cr ---- Si -·-·- Mn ·····. 1—Adding alloy agents or crop ends and scrap, 2—endpoint of blowing period I, 3—endpoint of blowing period II.

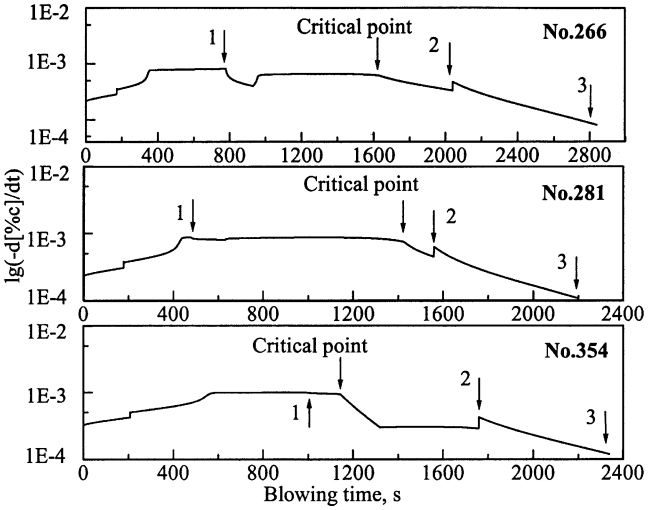

Fig. 2—Changes in decarburization rate (for three heats) predicted by the model with refining time. 1—Adding crop ends and scrap or alloy agents, 2—endpoint of blowing period I, 3—endpoint of blowing period II. Critical point: for 266, 1626 s and 6.1790×10^{-4} mass pct/s; for 281, 1425 s and 7.4102×10^{-4} mass pct/s; and for 354, 1143 s, 9.3923×10^{-4} mass pct/s.

of the bath composition and temperature. The latter are closely related to many factors, such as the kinetics of the refining process, the mass and heat balances, *etc.*

C. *Decarburization Rate and Critical Carbon Concentration*

Figure 2 demonstrates the changes in the decarburization rates for three heats (266, 281, and 354) during the refining process with time. With the blowing process progressing, the bath temperature rising, and x_c increasing, the decarburization rate gradually increases, attains a relatively stable value in a short time, and is proportional to the oxygen blowing rate (Eq. [5]). Under a constant oxygen flow rate, however, the decarburization is not constant, because x_C has nonlinearly been changing and increasing during the refining process. After the carbon content decreased to low levels and achieved the critical value, the decarburization changed into being controlled by the mass transfer of carbon in liquid steel. At this time, the decarburization rate is related to the carbon content (Eq. [9]). It must be pointed out that at high carbon levels, the carbon concentration in the steel can also influence the decarburization rate by changing x_C, although its role is smaller. When the decarburization process is controlled by the liquid-phase mass transfer of carbon, its rate also concerns the supplied oxygen rate, only its influence is greatly weakened. These are in accordance with the actual situations and are one more feature of the model.

The critical carbon concentration is determined by the thermodynamic and kinetic considerations in the process and system. Also, it is defined by the bath chemical composition and temperature, the activities of components, the partial pressure of carbon monoxide, the blowing rates of oxygen and inert gas, the stirring and mixing state of the bath, the reaction interface, the geometry of the reactor, *etc.* The critical carbon content fluctuates in the range of 0.1 to 0.6 mass pct for the oxygen converter process.[5,6,7] The values obtained by Roichel and Szekely[8] are 0.15 and 0.5 mass pct for the refining processes of austenitic stainless steel, respectively, in a 75-t VOD furnace and a 75-t AOD vessel. The results given by this model indicated that for the refining process of austenitic stainless steel in an 18-t AOD vessel, the critical carbon concentration is in the range of 0.25 to 0.40 mass pct. Considering the reasonability and reliability of the model and the use of the discriminant of $|dC_1/dt| < |dC_2/dt|$, the range obtained in the present work should also possess a higher precision.

D. *Changes in Composition and Temperature of Molten Steel*

The changes in the concentrations of C, Cr, Si, and Mn in the liquid steel and the bath temperature during the refining process (for heat 307) are given in Figure 3. It can be seen from this figure that, at the initial stage of the blowing process, the contents of C, Cr, Si, and Mn in the steel all decrease, although the bath temperature is relatively low. The loss rate of Si is the largest, and its oxidation reaction rapidly approaches a dynamic equilibrium and, essentially, no longer consumes oxygen. Simultaneously, the bath temperature quickly goes up, the loss rate of carbon subsequently increases, and the rate of Cr oxidation gradually decreases. The oxidation reaction of Mn approaches a dynamic equilibrium more quickly than that of Si, due to its lower deoxidization power, and is basically not influenced by the bath temperature and the oxidation or reduction extents of the other elements. The oxidation of carbon and chromium is accelerated with Si and Mn exiting the competition of consuming oxygen. Adding the crop ends and scrap or alloy agents (mainly high-carbon ferrochrome and nickel) makes the concentrations of C and Cr increase to a small extent and the bath temperature decrease in a short duration. However, the bath temperature rapidly goes up due to the additional losses of C and Cr. Hereafter, the carbon and chromium contents uninterruptedly decrease as the bath temperature continuously rises during the majority of the time of blowing period I, and their change rates nearly become stable. Simultaneously, the concentration of Mn (even Si) slightly rises

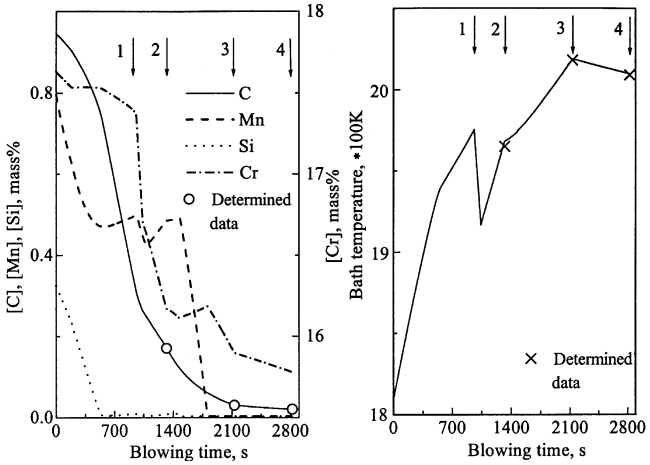

Fig. 3—Predicted changes in concentrations of C, Cr, Si, and Mn in liquid steel and bath temperature during the AOD refining process by the model (heat 307). 1—Adding crop ends and scrap or alloy agents; 2—endpoint of blowing period I; 3—endpoint of blowing period II; and 4—endpoint of blowing period III.

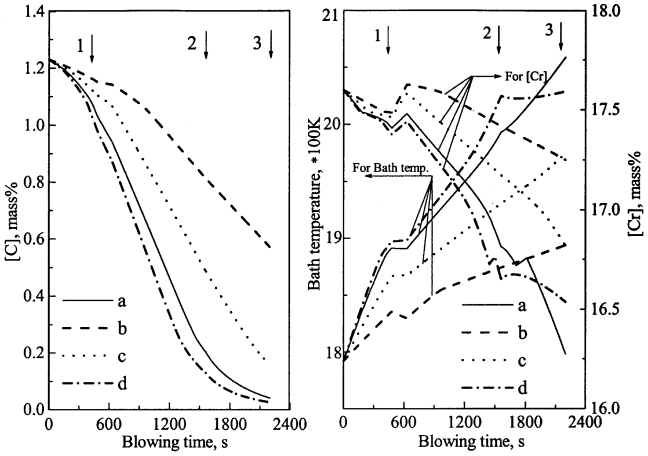

Fig. 4—Changes in concentrations of carbon and chromium in molten steel and bath temperature at given flow rates of oxygen and nitrogen (argon) and their ratio values for heat 281. 1—Adding alloy agents or crop ends and scrap; 2—endpoint of blowing period I; and 3—endpoint of blowing period II. a—O_2:N_2 = 800:400 (Nm^3/h) for blowing period I and O_2:Ar = 600:600 (Nm^3/h) for period II (existing practice). b—O_2:N_2 = 400:800 (Nm^3/h) for blowing period I and O_2:Ar = 400:800 (Nm^3/h) for period II. c—O_2:N_2 = 600:600 (Nm^3/h) for blowing period I and O_2:Ar = 600:600 (Nm^3/h) for period II. d—O_2:N_2 = 900:500 (Nm^3/h) for blowing period I and O_2:Ar = 200:800 (Nm^3/h) for period II.

again, owing to the reduction of a small amount of manganese oxide (or silica) in the dynamic equilibrium, then decreases to the lowest value of almost zero (Figure 3). The carbon content continues to reduce at a diminishing rate, and the chromium content sustains lowering at a progressively increasing rate after the critical point and during the blowing process of period II. Relevantly, the bath temperature moves up with steady steps. Throughout, there exists the competitive oxidation and reduction reactions among C, Cr, Si, and Mn. The changes in their concentrations and the bath temperatures occur just in this kind of competition.

E. *Influence of Blowing Gas Rate on Decarburization*

The blown gas flow rate is closely related to the oxidation of the elements in the bath and, undoubtedly, strongly influences the refining process. Choosing the optimal ratio of oxygen to argon (or nitrogen), thus making the blowing process progress smoothly and bringing about a decrease of the carbon while preserving the chromium, has always been an objective pursued by metallurgists for the AOD process.

As clearly shown in Figure 2, the critical point always arises before the end of blowing period I in the existing blowing practice. The surplus oxygen is almost all consumed for the oxidation of the chromium after the critical point. This means that the time of blowing period I is excessively long. This may lead to increasing the high consumption of reductants, slag materials, and oxygen, extending the treatment time and reducing the service life of the refractory lining. On the other hand, it is often demonstrated that the supplied oxygen before the critical point is insufficient in this practice. From the viewpoint of process optimization, obviously, this kind of blowing practice is not reasonable.

It can be suggested from the model predictions that, under the prerequisite of ensuring that violent splashing of the liquid on the bath surface does not take place, raising suitably the blowing flow rates of oxygen and nitrogen (or argon) will be beneficial to heightening the rising rate of the bath temperature and to intensifying the decarburization in blowing period I. For blowing period II, lowering appropriately the ratio of oxygen to argon may decrease the loss of Cr, thus avoiding an excessively high bath temperature. Also, the dilution role of argon to carbon monoxide and the agitation of the gas stream to the bath may be fully utilized, thus making the decarburization at low carbon levels progress smoothly.

Assuming a change of only the blowing mode and taking the additional three sets of different O_2:N_2 and O_2:Ar values from the existing practice for heat 281, modeling calculations have also been carried out using this model; the results are presented in Figure 4 and Table III, respectively.

It can clearly been seen from Figure 4 and Table III that, for the second blowing mode with O_2:N_2 = 400:800 (Nm^3/h) in blowing period I and O_2:Ar = 400:800 (Nm^3/h) in II blowing period II, the efficiency of decarburization is poor and the temperature of the bath is low, although the loss of chromium is very small. In the case of the third blowing mode, with O_2:N_2 = 600:600 (Nm^3/h) in blowing period I and O_2:Ar = 600:600 (Nm^3/h) in blowing period II, the effectiveness of decarburization is also not good, the carbon contents at the endpoints of blowing periods I and II are as high as approximately 0.49 and 0.16 mass pct, respectively, and the temperature is also on the low side. If using the fourth blowing operation, with O_2:N_2 = 900:500 (Nm^3/h) in blowing period I and O_2:Ar = 200:800 (Nm^3/h) in blowing period II, results much better than those with the existing blowing practice may be obtained, the carbon concentration of the blowing period II endpoint may be decreased to a lower value (0.0255 mass pct), and the corresponding chromium content is higher, with a bath temperature decrease of 30 K. This means that there may be a better efficiency of removing the carbon with preserving the chromium in this case.

Thus, adjusting continuously the ratios of the oxygen to nitrogen (argon) and their flow rates, in terms of the changes in the bath temperature and composition in the blowing process, to match the supplied gases to the demand of the

Table III. Refining Efficiencies Predicted by the Model at Different Blowing Modes for Heat 281

Blowing Mode, Nm^3/h	[C], Mass Pct		[Cr], Mass Pct		Temperature, °C	
	End of I Period	End of II Period	End of I Period	End of II Period	End of I Period	End of II Period
(1) Existing practice I period O_2:N_2 = 800:400 II period O_2:Ar = 600:600	0.2038	0.0405	16.8131	16.2744	1702.42	1785.48
(2) I period O_2:N_2 = 400:800 II period O_2:Ar = 400:800	0.8129	0.5709	17.4170	17.2491	1600.99	1620.75
(3) I period O_2:N_2 = 600:600 II period O_2:Ar = 600:600	0.4874	0.1586	17.1722	16.8146	1657.43	1702.21
(4) I period O_2:N_2 = 900:500 II period O_2:Ar = 200:800	0.1294	0.0255	16.6519	16.5365	1751.54	1755.50

refining reactions can effectively promote the decarburization process. Also, it can obviously decrease the consumption of gases and the loss of Cr and ensure going on smoothly to the followup treatment procedures. The model proposed and developed in the present work can offer a reliable control basis for this purpose.

Moreover, it can be pointed out that the other operating factors, such as the initial temperature and mass of liquid steel and the addition of crop ends, scrap, and alloy agents, *etc.*, can, to different degrees, directly influence the decarburization and other refining reactions too. All of those factors should reasonably be controlled. The model developed and proposed in the present work can also provide very useful and reliable information for these operations.

III. CONCLUSIONS

The new mathematical model for the AOD refining process proposed and developed in Part I of the present work has been applied to the austenitic stainless steel making in an 18-t AOD vessel and has been tested on data of 32 heats obtained in production. The following conclusions can be drawn from the results given by the model.

1. The carbon concentrations and bath temperatures at the endpoints of blowing periods calculated by the model are in excellent agreement with the determined data. The Cr content after the predeoxidization obtained from the model predictions also agrees very well with the observed value. The changes in the bath composition and temperature during the AOD refining process of stainless steel with time can be accurately predicted using this model.
2. The assumptions made to develop the model can well reflect the real situations in the AOD process.
3. There exists throughout competitive oxidation among the various elements during the refining process. The Gibbs free energies of the oxidation reactions of elements can be used to characterize fully this kind of competition and to determine reasonably the distribution ratios of oxygen among the elements.
4. The critical carbon concentration of decarburization (after which the decarburization changes into being controlled by the mass transfer of carbon in molten steel) for the AOD refining process of austenitic stainless steel in an 18-t AOD vessel is in the range of 0.25 to 0.40 mass pct.
5. The ratio of oxygen to argon (or nitrogen) and the blowing gas flow rate can strongly influence the changes in the bath composition and temperature. For the existing blowing mode of O_2:N_2 = 800:400 (Nm^3/h) in the first blowing period and O_2:Ar = 600:600 (Nm^3/h) in the second blowing period, appropriately raising the oxygen and nitrogen flow rates in the first period and decreasing the oxygen flow rate and increasing the supplied argon rate in the second blowing period can not only heighten the rising rate of the bath temperature and intensify the decarburization in the first period, but also reduce the loss of chromium, avoid the excessively high bath temperature, and remove the carbon in the liquid steel to a lower level in the second period.
6. Other operating factors, such as the initial temperature and mass of liquid steel, the addition of crop ends, scrap, and alloy agents, etc. can also change the decarburization progress. All of these factors should be reasonably controlled.
7. The model can provide some very useful information and a reliable basis for optimization of the technology of the AOD refining process of stainless steel and control of the process in real time and online.

ACKNOWLEDGMENTS

The authors gratefully acknowledge the support of the National Natural Science Foundation of China (Grant. No. 59474016). The Shanghai No. 5 Iron and Steel (Group) Corporation kindly offered the data on AOD heats.

REFERENCES

1. Ji-He Wei and De-Ping Zhu: *Metall. Mater. Trans. B*, 2002, vol. 33B, pp. 111-19.
2. H. Gorges, W. Pulvemacher, W. Rubens, and H. Diersten: *Proc. 3rd Int. Iron Steel Congr.*, Chicago, IL, Apr. 16–20, 1978, ASM INTERNATIONAL, Materials Park, OH, pp. 161-67.
3. F. Oeters: *Metallurgy of Steelmaking*, Verlag Stahleisen mbH, Berlin, Germany, 1994, ch. 8.
4. Ji-He Wei, Jin-Chang Ma, Yiang-Yi Fan, Neng-Weu Li, Sen-Long Yang, Shun-Hua Xing, and Deng-Ping Zhu: *Ironmaking and Steelmaking*, 1999, vol. 26 (5), pp. 363-71.
5. G. Breuer, G. Trömel, and H.J. Engell: *Arch. Eisenhüttenwes.*, 1968, vol. 39, pp. 553-57.
6. H. Nomura and K. Mori: *Trans. Iron Steel Inst. Jpn.*, 1973, vol. 13, pp. 325-32.
7. K. Koch, J. Sittard, and P. Valentin: *Arch. Eisenhüttenwes.*, 1976, vol. 47, pp. 583-88.
8. J. Reichel and J. Szekely: *Iron Steelmaker*, 1995, No. 5, pp. 41-48.